PARALLEL 3D FINITE ELEMENT PARTICLE-IN-CELL CODE FOR HIGH-FIDELITY RF GUN SIMULATIONS*

A. Candel†, A. Kabel, L. Lee, Z. Li, C. Limborg, C. Ng,
G. Schussman, R. Uplenchwar and K. Ko
SLAC, Menlo Park, CA 94025, USA

Abstract

SLAC's Advanced Computations Department (ACD) has developed the first high-performance parallel Finite Element 3D Particle-In-Cell code, Pic3P, for simulations of RF guns and other space-charge dominated beam-cavity interactions. As opposed to standard beam transport codes, which are based on the electrostatic approximation, Pic3P solves the complete set of Maxwell-Lorentz equations and thus includes space charge, retardation and wakefield effects from first principles. Pic3P uses advanced Finite Element methods with unstructured meshes, higher-order basis functions and quadratic surface approximation. A novel scheme for causal adaptive refinement reduces computational resource requirements by orders of magnitude. Pic3P is optimized for large-scale parallel processing and allows simulations of realistic 3D particle distributions with unprecedented accuracy, aiding the design and operation of the next generation of accelerator facilities. Applications to the Linac Coherent Light Source (LCLS) RF gun are presented.

INTRODUCTION

The Office of Science in the U. S. DOE is promoting the use of High Performance Computing (HPC) in projects relevant to its mission via the 'Scientific Discovery through Advanced Computing' (SciDAC) program which began in 2001 [1]. Since 1996, SLAC has been developing a parallel accelerator modeling capability, first under the DOE Grand Challenge and now under SciDAC, for use on HPC platforms to enable the large-scale electromagnetic and beam dynamics simulations needed for improving existing facilities and optimizing the design of future machines.

METHODS

In the following, a brief introduction to the employed methods for solving the full set of Maxwell's equations in time domain in the presence of charged particles is given.

Maxwell Finite Element Time-Domain

In our approach, Ampère's and Faraday's laws are combined and integrated over time to yield the inhomogeneous vector wave equation for the time integral of the electric field:

$$\varepsilon\frac{\partial^2}{\partial t^2}\int_{-\infty}^{\mathbf{t}}\mathbf{E}\,\mathrm{d}\tau+\nabla\times\mu^{-1}\nabla\times\int_{-\infty}^{\mathbf{t}}\mathbf{E}\,\mathrm{d}\tau=-\mathbf{J},\quad(1)$$

where $\mathbf{E}$ is the electric field intensity, $\mathbf{J}$ is the electric current source density, and ε and μ are the electric permittivity and magnetic permeability.

The computational domain is discretized into curved tetrahedral elements and $\int_{-\infty}^{t}\mathbf{E}\,\mathrm{d}\tau$ in Eq. (1) is expanded into a set of hierarchical Whitney vector basis functions $\mathbf{N_i}(\mathbf{x})$ up to order p within each element:

$$\int_{-\infty}^{t}\mathbf{E}(\mathbf{x},\tau)\,\mathrm{d}\tau=\sum_{i=1}^{N_p}e_i(t)\cdot\mathbf{N_i}(\mathbf{x}).\quad(2)$$

For illustration, $N_2=20$ and $N_6=216$. After accounting for boundary conditions at domain boundaries and between neighboring elements, a global number of expansion coefficients is obtained, representing the field degrees of freedom (DOFs) of the system.

Substituting Eq. (2) into Eq. (1), multiplying by a test function and integrating over the computational domain Ω results in a matrix equation, second-order in time. The unconditionally stable implicit Newmark-Beta scheme [2] is employed for numerical time integration. The resulting sparse positive definite system matrix is distributed over the compute nodes and is either factorized with a direct solver for smaller problems, or the linear system is solved iteratively at each time step with a conjugate gradient method with suitable preconditioners.

At a given moment in time, the electric field $\mathbf{E}$ and the magnetic flux density $\mathbf{B}$ are then easily obtained from the solution vector $\mathbf{e}$:

$$\mathbf{E}(\mathbf{x})=\sum_{\mathbf{i}}(\partial_{\mathbf{t}}\mathbf{e})_{\mathbf{i}}\cdot\mathbf{N_i}(\mathbf{x})\quad(3)$$

and

$$\mathbf{B}(\mathbf{x})=-\sum_{\mathbf{i}}(\mathbf{e})_{\mathbf{i}}\cdot\nabla\times\mathbf{N_i}(\mathbf{x}).\quad(4)$$

* Work supported by the U.S. DOE ASCR, BES, and HEP Divisions under contract No. DE-AC002-76SF00515.
† candel@slac.stanford.edu

Particle-In-Cell (PIC)

Numerical charge conservation is critical during the self-consistent simulation of charged particles and electromagnetic fields. If the discrete analogs of the two Maxwell divergence equations $\nabla \cdot \mathbf{B} = \mathbf{0}$ and $\nabla \cdot \mathbf{E} = \rho$ are satisfied at $t = 0$, then it is sufficient to fulfill the discrete versions of wave Eq. (1) and the continuity equation

$$\frac{\partial \rho}{\partial t} + \nabla \cdot \mathbf{J} = \mathbf{0}$$

in order to maintain charge conservation at all times. In our approach, these conditions are satisfied by using Whitney basis functions and starting with a charge-free simulation domain.

Freely moving charges are modeled by a number of macro particles specified by position $\mathbf{x}$, momentum $\mathbf{p}$, rest mass m and charge q attributes. The total current density is then approximated as

$$\mathbf{J}(\mathbf{x}, t) = \sum_i \rho(\mathbf{x} - \mathbf{x_i}, t) \cdot \mathbf{v_i}(t),$$

with $\mathbf{v} = \frac{\mathbf{p}}{\gamma m}$, $\gamma^2 = 1 + |\frac{\mathbf{p}}{mc}|^2$ and ρ the macro particle charge density, currently implemented for point charges and Gaussian line currents (which act as smoothing filter). The macro particles obey the classical relativistic collisionless (Newton-Lorentz) equations of motion,

$$\begin{aligned} \frac{d\mathbf{r}}{dt} &= \mathbf{v}, \\ \frac{d\mathbf{p}}{dt} &= q(\mathbf{E} + \mathbf{v} \times \mathbf{B}), \end{aligned}$$

which are integrated using the standard 'Boris' pusher, an explicit method splitting the momentum update into two accelerations and one rotation [3].

Causal Moving Window

FE methods are most efficient when using (adaptive) hpq-refinement, where h stands for the mesh resolution, p for the polynomial order of the basis functions and q for the degree of mesh curvature. Our current implementation supports static h- and q-refinement (q=1,2) as well as adaptive p-refinement (p=0...6), where each element is assigned an independent value of p and its basis functions that are shared with neighboring elements are restricted to the highest common order. This requires a consistent set of hierarchical FE basis functions.

Higher-order elements not only significantly improve field accuracy and dispersive properties [4], but they also generically lead to higher-order accurate particle-field coupling equivalent to, but much less laborious than, complicated higher-order interpolation schemes commonly found in finite-difference methods.

Orders of magnitude in computational resources can be saved, while preserving full simulation accuracy, by restricting higher-order p-refinement to regions that are inside the causal range of the particle bunch. Since a change of the selected basis functions requires reassembly of the system matrix, adaptive p-refinement is usually only done from time to time, in accordance with the particle dynamics. Fig. 1 shows a Minkowski spacetime diagram indicating the causal domain for a bunch transiting through a compact structure. The causal domain can be determined from the bunch emission and exit spacetime positions, and non-causal fields are neglected by not including their elements in the computation. A resulting parallel partitioning after dynamic load balancing is shown in Fig. 2.

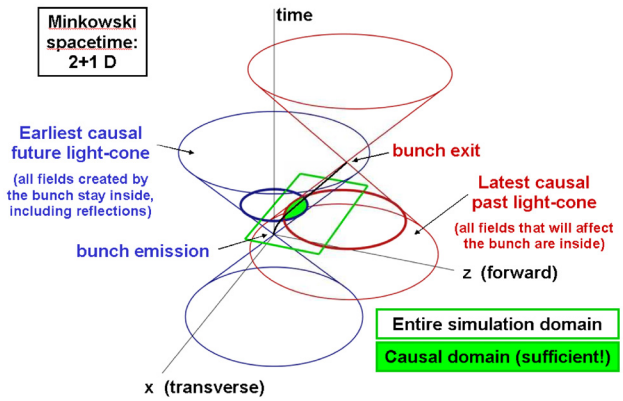

Figure 1: 2+1D spacetime diagram indicating the causal field domain for an accelerated particle bunch inside the gun at a snapshot in time.

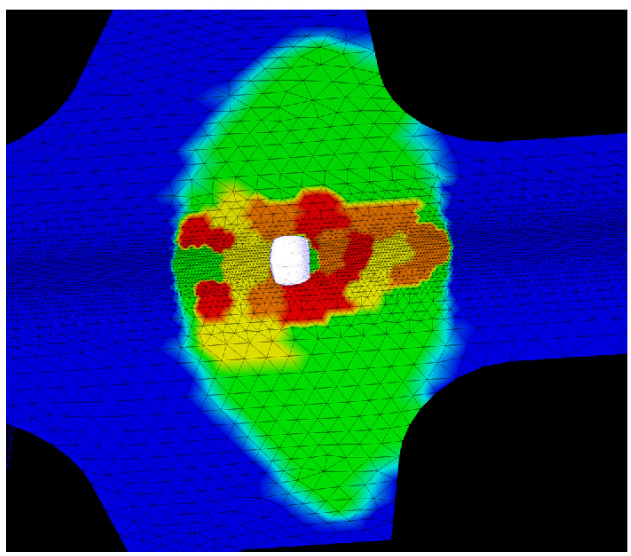

Figure 2: Example of a Pic3P simulation employing the causal moving window technique. Elements outside the causal domain are neglected in the field computations and are indicated by the blue color. Elements and fields in the causal domain are partitioned onto all CPUs with dynamic load balancing and are indicated by different colors. Macro particles are distributed among all CPUs and are shown in white.

RESULTS

PIC simulations of the 1.6 cell S-band LCLS RF gun are presented [5]. In the simulations, the gun is driven by the π-mode with a peak accelerating field gradient of 120 MV/m at the cathode (the cavity wall). A cold, uniform, 10 ps long (flat-top), cylindrically symmetric electron bunch of 1 mm radius is emitted, centered around a phase of -58° with respect to the crest. Solenoidal focusing fields are neglected for simplicity. These parameters allow comparisons between the 3D codes Pic3P and PARMELA and the 2D codes Pic2P and MAFIA.

For Pic3P simulations, a conformal, unstructured 3D (1/4) mesh model with 305k tetrahedral elements is used, with h-refinement along the beam trajectory. High fidelity cavity modes are obtained with ACD's parallel FE frequency domain code Omega3P and directly loaded into Pic3P. Fig. 3 shows the evolution of the normalized transverse RMS emittance during transit through the gun for different bunch charges. There is excellent agreement between Pic3P and the 2D results from Pic2P and MAFIA, as expected from the high cylindrical symmetry in the fields and the convergence behavior of the codes. PARMELA results differ as space charge effects are significant, presumably because it ignores wakefield and retardation effects, as detailed in a previous study[6]. By using the causal window technique in Pic3P (cf. Fig. 1 and 2), the problem size was reduced by one order of magnitude without a loss of simulation accuracy. Note that Pic3P is able to solve problems that are several hundred times larger than what is needed here in order to reach convergence in the bunch emittance. Parallel dynamic load balancing and excellent scalability to thousands of CPUs result in fast turn-around times. Results on large-scale, realistic 3D simulations have been presented in the past [7].

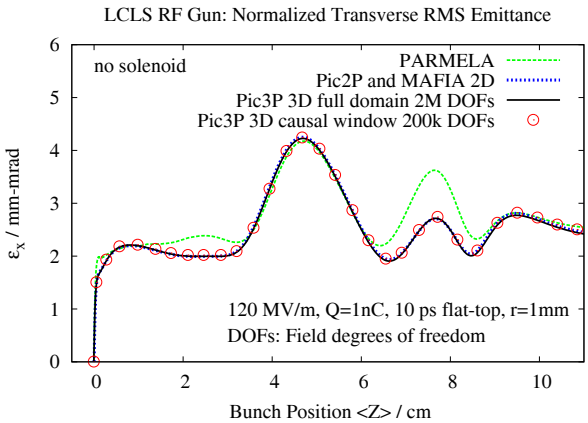

Figure 3: Comparison of normalized transverse RMS emittance as a function of beam position in the LCLS RF gun as calculated by PARMELA, Pic2P and MAFIA 2D (both agree), and Pic3P, where the causal window technique reduces the problem size by one order of magnitude.

CONCLUSIONS

The parallel Finite Element 3D electromagnetic PIC code Pic3P, the first such successful implementation, was used to model space charge effects in the LCLS RF gun from 1st principles, including space charge, wakefield and retardation effects. On a cylindrically symmetric benchmark case, Pic3P shows excellent agreement with 2D codes such as MAFIA and Pic2P. Results from the electrostatic code PARMELA differ as wakefield and retardation effects are neglected.

Pic3P employs state-of-the-art parallel Finite Element methods on conformal, unstructured meshes with unconditionally stable time integration and self-consistent higher-order particle-field coupling. In combination with novel causal moving window techniques and dynamic load balancing, Pic3P allows parallel 3D PIC simulations of high-brightness, low-emittance electron injectors with unprecedented accuracy, aiding the design and operation of the next generation of accelerator facilities.

ACKNOWLEDGMENTS

This work was supported by the U.S. DOE ASCR, BES, and HEP Divisions under contract No. DE-AC002-76SF00515. This research used resources of the National Energy Research Scientific Computing Center, which is supported by the Office of Science of the U.S. Department of Energy under Contract No. DE-AC02-05CH11231. We also acknowledge the contributions from our SciDAC collaborators in numerous areas of computational science.

REFERENCES

[1] Cho Ng et al., "Design and Optimization of Large Scale Accelerator Systems through High-Fidelity Electromagnetic Simulations", Invited Talk given at SciDAC 2008 Conference, Seattle, Washington, July 13-17, 2008.

[2] N. M. Newmark, "A method of computation for structural dynamics", Journal of Eng. Mech. Div., ASCE, vol. 85, pp. 67-94, July 1959.

[3] J. P. Boris, "Relativistic plasma simulation-optimization of a hybrid code", Proc. Fourth Conf. Num. Sim. Plasmas, Naval Res. Lab, Wash. D.C.,pp. 3-67, Nov. 2-3, 1970.

[4] M. Ainsworth, "Dispersive properties of high-order Nedelec/edge element approximation of the time-harmonic Maxwell equations", Philos. trans.-Royal Soc., Math. phys. eng. sci., vol. 362, no. 1816, pp. 471-492, 2004.

[5] L. Xiao et al., "Dual Feed RF Gun Design for the LCLS", Proc. PAC 2005, Knoxville, Tennessee, May 15-20, 2005.

[6] A. Candel et al., "Parallel Higher-order Finite Element Method for Accurate Field Computations in Wakefield and PIC Simulations", Proc. ICAP 2006, Chamonix Mont-Blanc, France, October 2-6, 2006.

[7] A. Candel, "Parallel 3D Finite Element Particle-In-Cell Simulations for the LCLS RF Gun", LCLS Seminar Talk, Stanford Linear Accelerator Center, March 25, 2008.